Finite-element analysis of a piled embankment with reinforcement and subsoil

Zhuang, Y; Ellis, EA

Published in:
Géotechnique

DOI:
10.1680/jgeot.15.P.139

Publication date:
2016

Finite-element analysis of a piled embankment with reinforcement and subsoil

Y. Zhuang (Geotechnical Research Institute, College of Civil and Transportation Engineering, Hohai University, Nanjing, China)

E.A. Ellis (University of Plymouth, Plymouth, UK)

Published version available at:

http://www.icevirtuallibrary.com/doi/full/10.1680/jgeot.15.P.139

Abstract

Zhuang & Ellis (2014) considered predictions of reinforcement tension in a piled embankment from BS 8006 (BSI, 2010 and 2012), comparing the results with finite element model predictions. In keeping with BS 8006 any contribution from the subsoil beneath the embankment was ignored.

This paper extends that work by also considering the potentially beneficial contribution of a lightly overconsolidated clay subsoil layer, both in the finite element predictions and as a simple modification to the BS 8006 predictive method. It is assumed that there is no 'working platform' (granular) material below the pile cap level, and that the water table in the subsoil does not drop, since either of these factors would be likely to significantly reduce the ability of the subsoil to carry load from the embankment.

As anticipated the subsoil support reduces reinforcement tension. When compared to the finite element results the proposed modified BS 8006 prediction is quite accurate. The BSI (2012) modified prediction is 'best' (but sometimes slightly unconservative), whilst the BSI (2010) modified prediction is conservative in all cases considered.

Notation

a = (square) pile cap size (m)

A = variable related to reinforcement stiffness and pile cap geometry and spacing (Equation 4) (kN/m^2)

b = (square) pile size (m)

c' = cohesion intercept (kN/m^2)

H_e = embankment height (m)

H_s = subsoil thickness (m)

J = long-term secant stiffness (at appropriate strain) for reinforcement (kN/m run (or MN/m))

k_s = the 'subgrade reaction' at the surface of the subsoil (kN/m^2/m)

s = pile centre-to-centre spacing (for piles on a square grid) (m)

T_{rp} = maximum tensile load in reinforcement (kN/m run)

W_T = distributed (vertical) load carried by reinforcement between adjacent pile caps (kN/m)

y = maximum sag in reinforcement (m)

α = dimensionless variable (Equation 5)

δ = interface friction angle (degrees)

ε = strain in reinforcement (dimensionless)

v = Poisson ratio

σ_e = the vertical stress at the base of the embankment (including the effect of arching) (kN/m^2)

σ_r = the vertical stress carried by the reinforcement (kN/m^2)

σ_s = the vertical stress carried by the subsoil (kN/m^2)

$\Delta\sigma_v$ = increment of total stress in the subsoil (also increment of effective following consolidation) (kN/m^2)

$\Delta\sigma_{vp}$ = the increment of stress to reach the preconsolidation stress in the subsoil (kN/m^2).

φ' = friction angle (degrees)

1 Introduction

Zhuang & Ellis (2012) reported three-dimensional Finite Element (3D FE) modelling of arching in an unreinforced piled embankment, dependent on key geometrical variables (Figure 1):

a = the square pile cap dimension

s = the centre-centre pile spacing for a square grid

H_e = the embankment height

Zhuang & Ellis (2014) considered predictions of reinforcement tension in a piled embankment from BS 8006 (BSI, 2010 and 2012), comparing the results with 3D FE results. Based on BS 8006 any contribution from the subsoil beneath the embankment was ignored.

Han & Gabr (2002) performed a numerical study on reinforced piled embankments, including underlying subsoil. However, an axisymmetric analysis was used. Stewart & Filz (2005) also considered the effect of subsoil using numerical analysis, concluding that this should be a factor in design, but without considering how this might be achieved. EBGEO (2011) and Van Eekelen et al (2012) considered elastic response of the subsoil in analytical models. However, the models are complex, and the potentially very important effect of the subsoil preconsolidation stress is not considered.

This technical note extends the 3D FE studies of Zhuang & Ellis (2012 and 2014), also considering the contribution of a lightly overconsolidated subsoil layer. It is assumed that there is no 'working platform' (granular) material below the pile cap level, and that the water table in the subsoil does not drop, since either of these factors would be likely to significantly reduce the ability of the subsoil to support the embankment.

Simple modifications to the BS 8006 method for prediction of reinforcement tension are proposed to account for the subsoil contribution, and are compared with the 3D FE results.

2 Calculation of reinforcement tension including the effect of subsoil

2.1 Solution for components of vertical stress at the base of the embankment

It is assumed that the tensile reinforcement and subsoil act together to support the base of an arching embankment (Figure 1(a)):

$$\sigma_e = \sigma_r + \sigma_s$$

Equation 1

where

σ_e = the vertical stress at the base of the arching embankment

σ_r = the vertical stress carried by the reinforcement

σ_s = the vertical stress carried by the subsoil

The values will vary with plan location, but consideration of average values will satisfy equilibrium. Each of these three components will be considered in turn below.

Zhuang & Ellis (2014) concluded that the Hewlett and Randolph (1988) approach for determination of 'maximum arching' in the embankment (σ_e) shows most promise in BS 8006, and it will be used here. Zhuang et al (2012) noted that maximum arching is reached at relatively small subsoil settlement, hence variation of σ_e with settlement is not explicitly considered.

Proceeding to the reinforcement contribution from tensile reinforcement, Abusharar et al (2009), Ellis & Aslam (2009), Ellis et al (2010), and Zhuang et al (2014) have suggested that σ_r can be expressed in the form:

$$\sigma_r = A\left(\frac{y}{s-a}\right)^3$$

Equation 2

where

y = the maximum sag of the reinforcement between pile caps (normalised by the clear spacing between pile caps, s-a)

A is a variable with units kN/m^2 (see Appendix A)

Finally, the 'elastic' subsoil response (limited by the preconsolidation stress) can be written as

$$\sigma_s = k_s y \leq \Delta\sigma_{vp}$$

Equation 3

where

y = the settlement of the subsoil (which will vary with plan location, but will be taken as the maximum value, for compatibility with maximum sag in the reinforcement)

k_s = the 'subgrade reaction' at the surface of the subsoil (kN/m^2/m, eg. van Eekelen et al, 2012)

$\Delta\sigma_{vp}$ = the increment of stress on the subsoil to reach the preconsolidation stress

To 'solve' Equation 1, it is necessary to establish how σ_e (from the Hewlett and Randolph method) is distributed between σ_r and σ_s using compatibility of y (Equations 2 and 3). Iteration is readily automated on a PC. If the limit $\sigma_s = \Delta\sigma_{vp}$ is reached in Equation 3, then σ_r is independent of y:

$$\sigma_r = \sigma_e - \Delta\sigma_{vp}$$

Equation 4

2.2 Determination of W_T and T_{rp}

Once σ_r has been determined, further analysis is required to determine the tension in the reinforcement. Zhuang & Ellis (2014) discuss the distributed (vertical) load carried by the reinforcement between pile caps (W_T, kN/m) in BS 8006 (BSI 2010 and 2012). The corresponding equations will be written as

$$W_T = \alpha s \, \sigma_r$$

Equation 5

where

$\alpha = 1$ (BSI, 2010)

$\alpha = (s + a)/2s$ (BSI, 2012)

noting that the 2010 version is not current, and is not consistent with vertical equilibrium, but that the 2012 version predicts lower load (since $\alpha < 1$).

Zhuang & Ellis (2014) then considered derivation of the reinforcement tension (T_{rp}, kN/m run) from W_T, proposing

$$T_{rp} = W_T \frac{(s-a)}{2a} \left(1 + \frac{J}{6T_{rp}}\right)^{0.5}$$

Equation 6

where J is an appropriate long-term secant stiffness for the reinforcement (kN/m), which includes the effect of creep. Iteration is required since T_{rp} appears on both sides of the equation.

3 Finite element analyses

Figure 2 shows a schematic of the FE model, based on the boundaries shown in Figure 1(b). The approach is the same as Zhuang & Ellis (2012 and 2014), but explicitly modelling the subsoil, pile cap and pile. Table 1 summarises the analyses undertaken. Meshes contained approximately 35 to 190 thousand elements, and the sensitivity to mesh size was checked similar to Zhuang & Ellis (2014).

Constitutive modelling of the embankment as a dry elastic-perfectly plastic material was identical to Zhuang & Ellis (2012 and 2014), Table 2.

Like Zhuang & Ellis (2014), a single layer of biaxial tensile reinforcement was positioned 100 mm above the base of the embankment. Compared to separate 'upper' and 'lower' orthogonal layers, the tension result corresponds to an 'average', which would be more than an upper layer and less than a lower layer (Love & Miligan, 2003).

The 10.0 m thick soft subsoil was modelled using Modified Cam Clay (MCC; Wood, 1990), Table 3, with hydrostatic groundwater pressure from the water table at the surface of the subsoil. It was assumed that the clay had previously experienced a small vertical 'preconsolidation stress' ($\Delta\sigma_{vp}$) of 10 kN/m^2 in excess of the insitu vertical effective stress.

The pile cap and pile were modelled as an elastic material (concrete) with Young's Modulus of 30 GN/m^2, and Poisson's Ratio of 0.20. They were assumed to be either 'smooth' or 'rough' in terms of the interface friction angle with the surrounding soil (δ):

Smooth: $\delta = 0^o$

Rough: $\delta = 10^o$ for the subsoil (clay); $\delta = 15^o$ for the (granular) embankment material (on the top face of the cap)

At the start of the analyses only the subsoil, pile cap and pile were present. The insitu effective stress in the subsoil was specified based on the MCC parameters and preconsolidation stress.

The embankment was then constructed in layers, similar to Zhuang & Ellis (2012 and 2014). During this process the soft clay subsoil was treated as 'undrained' (considered pragmatic and conservative). The clay subsoil was then allowed to consolidate via drainage at the top and bottom boundaries.

.

Monitoring of pore water pressure confirmed that the anticipated excess pore pressure (γH_e) was generated during construction, and had completely dissipated by the end of the analysis (and hence the increase in total and effective stress in the layer were equal). Likewise, no sag or settlement occurred in the reinforcement during construction, but these values reached constant maxima by the end of consolidation.

4. Results for the subsoil

Forty-two FE analyses are reported, from the 21 combinations of geometry and reinforcement stiffness in Table 1, each for smooth and rough piles. Figure 3 shows the subsoil vertical stress increment ($\Delta\sigma_v$) and settlement (y) at the end of the analysis. As anticipated, increasing pile spacing (s) and embankment height (H_e) caused $\Delta\sigma_v$ and y to increase - data points for the largest s (= 3.5 m) are labelled in Figure 3(b).

'1-D prediction' lines are also shown, corresponding to purely vertical deformation, and uniform settlement with plan location. The 'elastic' one-dimensional subsoil stiffness (E'_0) was inferred from the MCC parameters, increasing approximately linearly from 0.20 MN/m^2 at the top of the subsoil layer to 2.55 MN/m^2 at the base. For $\Delta\sigma_v > \Delta\sigma_{vp}$ a nominal reduction in stiffness is shown, corresponding to the ratio $\lambda/\kappa = 3$.

Figure 3(a) shows the response at mid depth of the subsoil (5.0 m), where settlement was uniform with plan location (except very locally near a rough pile). The smooth pile results show good agreement with the '1-D prediction', whilst the rough pile results are slightly stiffer (due to the beneficial effect of negative skin friction in this respect).

In contrast, settlement was highly non-uniform near the surface of the subsoil layer. $\Delta\sigma_v$ and y were both maximum at the centre of a diagonal span between pile caps, and tended to zero at the pile cap. Figure 3(b) shows the response at the surface of the subsoil, now plotting the maxima of $\Delta\sigma_v$ and y. The '1-D prediction' line now corresponds to Equation 3, but noting that these equations were based on the concept average stress.

The maxima of $\Delta\sigma_v$ and y are somewhat stiffer than the 1-D prediction, and this was attributed to the localised shear strain resembling a bearing capacity mechanism observed near the surface of the subsoil. Again the rough pile gives stiffer response, but the effect is now relatively modest.

5. Results for reinforcement tension and conclusion

The general distribution of tension in the reinforcement was similar to Zhuang & Ellis (2014). Figure 4 shows the increase in *maximum* reinforcement tension (T_{rp}) with embankment height (H_e) in the same format as Zhuang & Ellis (2014).

A total of four prediction lines are shown, and denoted as follows (eg. 'H&R (2010) NSS'):

'H&R' is Hewlett & Randolph (1988) predictions of embankment arching, used throughout.

'2010' or '2012' refers to revisions of BS 8006 (BSI 2010 and 2012) in Equation 5.

'NSS' denotes 'No Subsoil Support' (from Zhuang & Ellis (2014)), whereas 'SS' denotes 'Subsoil Support' (Equation 3).

SS implies use of Equation 3, with k_s = 93 kN/m^2/m (based on the inferred subsoil E_0' profile); or $\Delta\sigma_{vp}$ = 10 kN/m^2 in Equation 4. In Figure 3(b) some FE results indicate $\Delta\sigma_v > \Delta\sigma_{vp}$, but a pragmatic design approach would ignore this.

In fact the $\Delta\sigma_{vp}$ = 10 kN/m^2 limit was reached in the majority of prediction cases. However, it was not in Figures 4(b) and (d), where the reinforcement response was relatively 'stiff' for low *s* and high *J*, and hence load on the subsoil was reduced.

Three sets of FE data points are shown and denoted as follows (eg. 'FE SS sm'):

'NSS' ('No Subsoil Support') again refers to Zhuang & Ellis (2014), whereas 'SS' ('Subsoil Support') refers to the new analyses reported here.

The SS analyses are either 'sm' or 'ro', referring to a 'smooth' or 'rough' pile respectively.

As anticipated, the effect of subsoil support is to reduce both the predictions of reinforcement tension and the FE results (where the rough pile slightly enhances this effect).

The FE data is between 4 % and 50 % lower than the BS 8006 (2010) prediction including the proposed modification for subsoil support. Meanwhile the FE data is between 41 % lower and 15 % higher than the BS 8006 (2012) prediction including the proposed modification for subsoil support. Where the FE data is significantly lower than the prediction (expressed as a percentage), this is for low tension (and low H_e).

As noted in Zhuang & Ellis (2014) there are arguments that the component Equations under- and over-predict various aspects of the behaviour. Nevertheless, the ultimate prediction of T_{rp} (including modification for subsoil support) is quite good compared to the FE data. The BS 8006 (2012) modified prediction is 'best' (but sometimes slightly unconservative), whilst the BS 8006 (2010) modified prediction is conservative in all cases considered.

References

Abusharar, S.W., Zheng, J.-J., Chen, B.-G. & Yin, J.-H. (2009). A simplified method for analysis of a piled embankment reinforced with geosynthetics. Geotextiles and Geomembranes 27, 39-52.

BSI (2010). BS 8006-1: Code of practice for strengthened/reinforced soils and other fills. London, UK: British Standards Institution.

BSI (2012). BS 8006-1: Code of practice for strengthened/reinforced soils and other fills, incorporating Corrigendum 1. London, UK: British Standards Institution.

EBGEO (2011). Recommendations for Design and Analysis of Earth Structures using Geosynthetic Reinforcements.

Ellis, E. A. & Aslam, R. (2009). Arching in piled embankments: comparison of centrifuge tests and predictive methods – part 2 of 2. Ground Engng 42, July, 28–31.

Ellis, E. A., Zhuang, Y., Aslam, R., Yu, H. S. (2010). Discussion of 'A simplified method for analysis of a piled embankment reinforced with geosynthetics' by Abusharar, Zheng, Chen and Yin, Geotextiles and Geomembranes 27, 39-52. Geotextiles and Geomembranes 28, 133-134.

Han, J. & Gabr, M. A. (2002). Numerical analysis of geosynthetic reinforced and pile-supported earth platforms over soft soil. J. Geotech. Geoenviron. Eng., 128(1), 44-53.

Hewlett, W. J. & Randolph, M. F. (1988). Analysis of piled embankments. Ground Engng 21, April, 12–18.

Love, J. & Milligan, G. (2003). Design methods for basally reinforced pile-supported embankments over soft ground. Ground Engng 39, March, 43–43.

Stewart, M.E. & Filz, G.M. (2005). Influence of clay compressibility on geosynthetic loads in bridging layers for column-supported embankment. Contemporary Issues in Foundation Engineering, pp.1-14.

Van Eekelen, S. J. M., Bezuijen, A., Lodder, H.J. & van Tol, A. F. (2012). Model experiments on piled embankments, part II. Geotextiles and Geomembranes 32, 82–94.

Wood, D. M. (1990). Soil Behaviour and Critical State Soil Mechanics. Cambridge University Press.

Zhuang, Y., Ellis, E. A. & Yu, H. S. (2012). Technical note: Three-dimensional finite-element analysis of arching in a piled embankment. Geotechnique 62, No. 12, 1127–1131.

Zhuang, Y., & Ellis, E. A. (2014). Finite-element analysis of a piled embankment with reinforcement compared with BS 8006 predictions. Geotechnique 64, No. 11, 910–917.

Zhuang, Y., Kang, Y.W. & Liu, H.L. (2014). A simplified model to analyze the reinforced piled embankments. Geotextiles and Geomembranes 42, 154–165.

Tables

Table 1 – Geometry and reinforcement stiffness

Pile cap, a: m	C-C cap spacing, s: m	Embankment height, H_e: m	Reinforcement stiffness, J: MN/m
1.0	2.0	2.0, 6.5, 10.0	1.0, 3.0
0.5	1.25	1.5, 3.5, 6.5	1.0, 3.0
1.0	2.5	3.0, 6.5, 10.0	3.0, 10.0
1.0	3.5	5.0, 6.5, 10.0	10.0

Table 2 – Material parameters for embankment fill

Unit weight, γ (kN/m^3)	Initial earth pressure coefficient, K_0	Young's Modulus (MN/m^2)	Poisson's Ratio, v	Cohesion intercept, c' (kN/m^2)	Friction angle, φ' (deg)	Kinematic dilation angle at yield (deg)
17.0	0.50	25	0.20	1	30	0

Table 3 – Material parameters for subsoil

λ	κ	Γ	M	Elastic Poisson's Ratio, v
0.30	0.10	3.30	0.772	0.20

Appendix A – Compatibility equation for tensile reinforcement

Equation 5 in Zhuang & Ellis (2014)

$$T_{rp} \approx 0.35\ J^{1/3} \left[W_T \left(\frac{s-a}{a}\right)\right]^{2/3}$$

Equation 8 in Zhuang & Ellis (2014)

$$\frac{y}{s-a} = \left(\frac{3T_{rp}}{4J}\right)^{0.5}$$

Eliminating T_{rp} between the two equations and re-arranging

$$7.4J\left(\frac{y}{s-a}\right)^3 \approx W_T \left(\frac{s-a}{a}\right)$$

Substituting $W_T = \alpha s \sigma_r$ (Equation 5 in main text) and re-arranging:

$$\sigma_r \approx \frac{7.4}{\alpha}\frac{a}{s}\frac{J}{(s-a)}\left(\frac{y}{s-a}\right)^3 = A\left(\frac{y}{s-a}\right)^3$$

$$A = \frac{7.4}{\alpha}\frac{a}{s}\frac{J}{(s-a)}$$

A has units kN/m^2

σ_r will vary with plan location, but is here nominally considered to be an 'average' value satisfying vertical equilibrium in Equation 1.

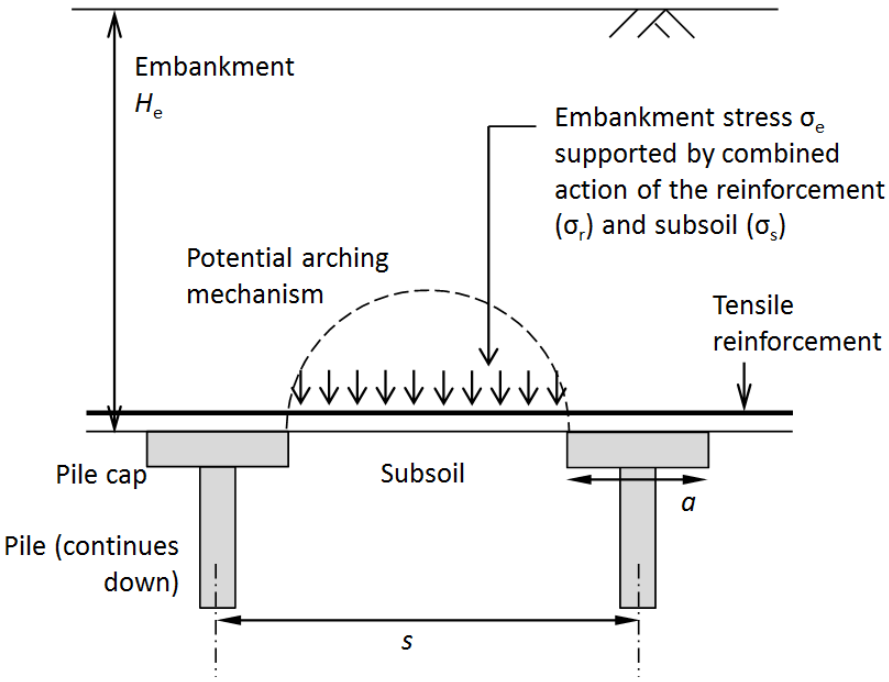

(a) Schematic of behaviour and geometry (vertical section through pile caps)

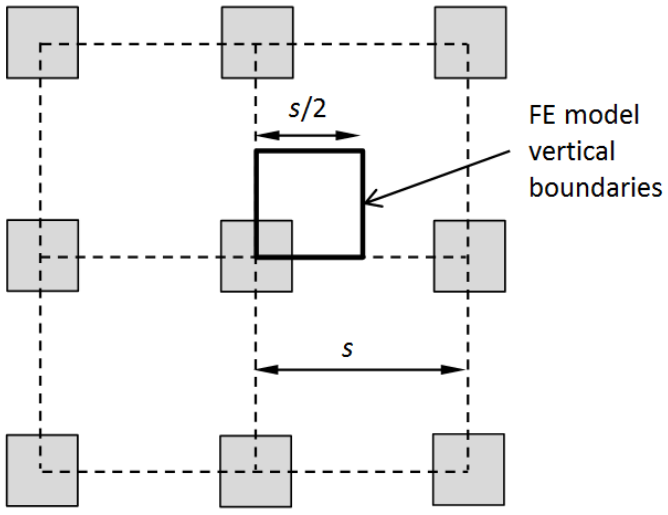

(b) FE model boundaries, one quarter of 'unit cell' (plan view)

Figure 1 – Piled embankment illustrating behaviour and FE model boundaries

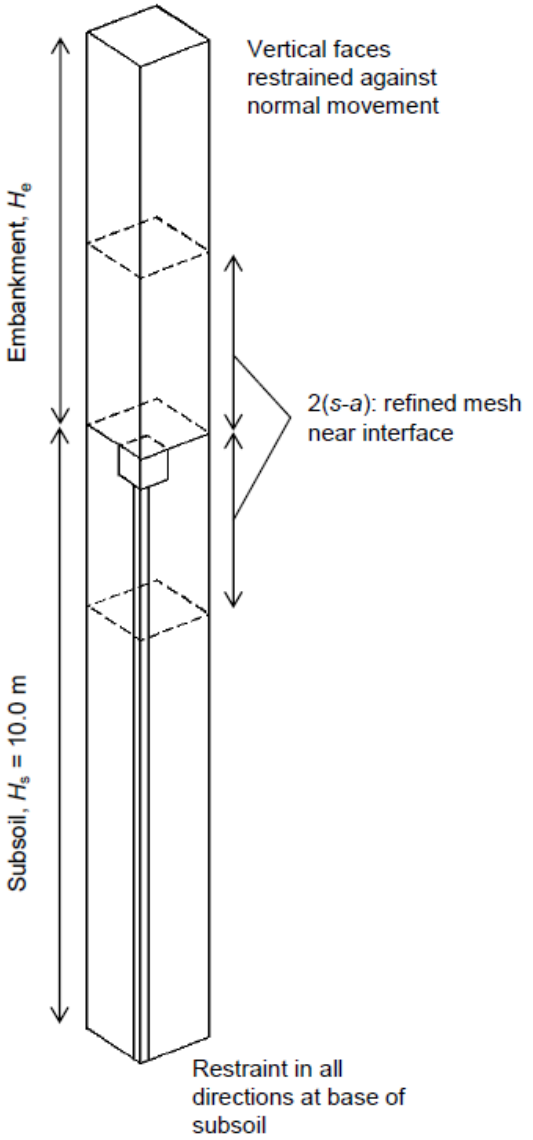

(a) Overview

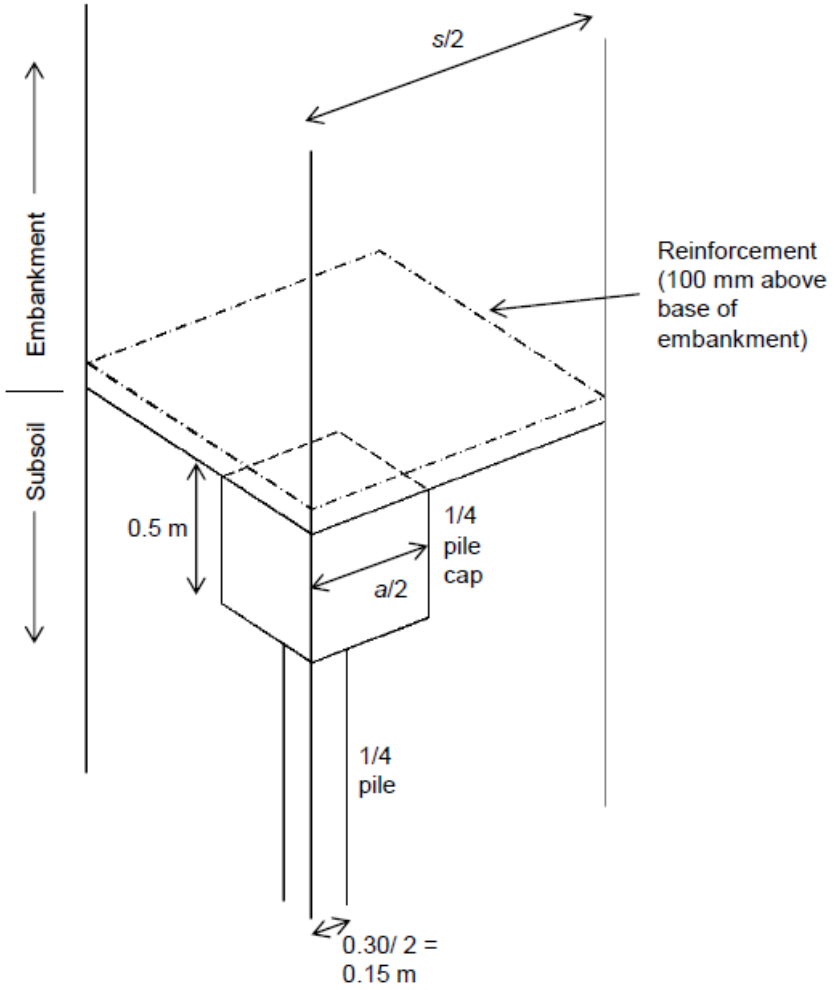

(b) Enlarged detail at embankment/ subsoil interface

Figure 2 - Finite element mesh geometry

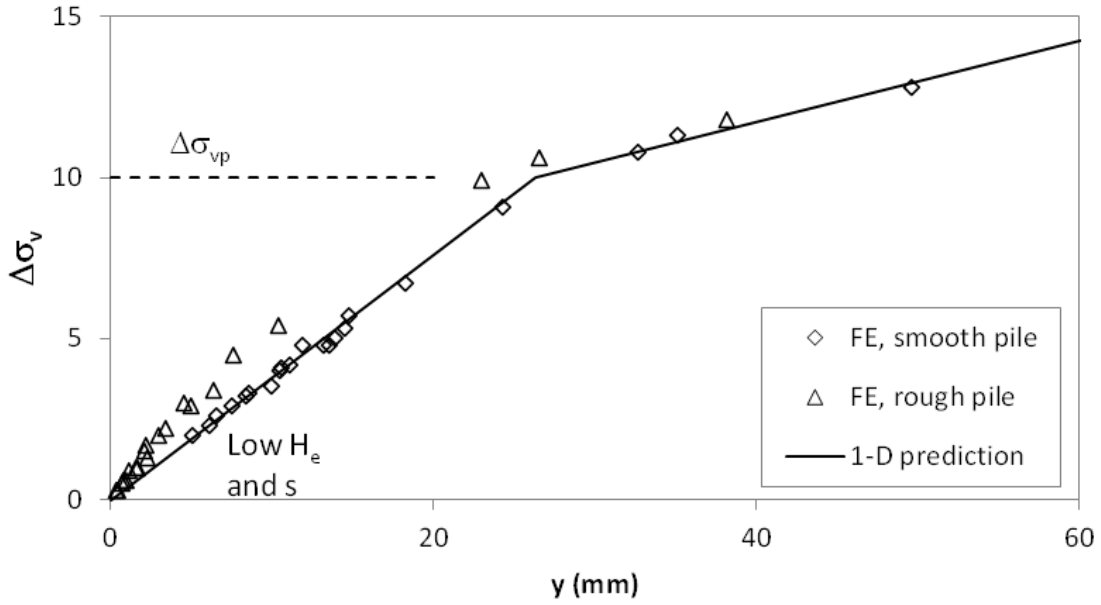

(a) z = 5 m (subsoil mid-depth)

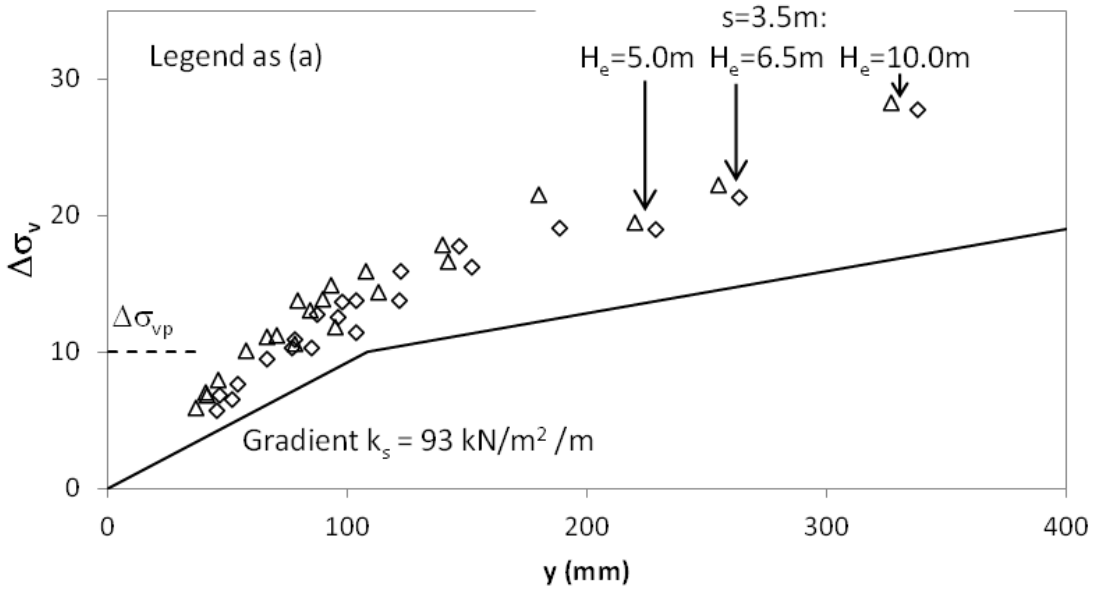

(b) z = 0 m (subsoil surface, maximum values at centre of diagonal span)

Figure 3 - Subsoil settlement (y) and stress increment ($\Delta\sigma_v$)

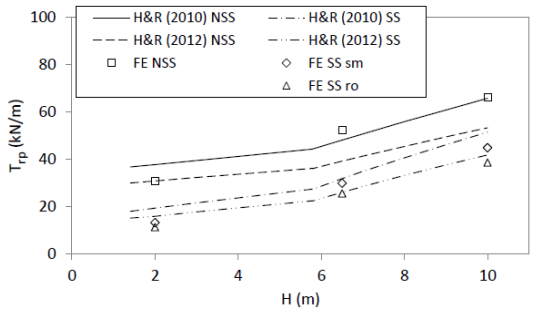

(a) a = 1.0 m, s = 2.0 m, J = 1.0 MN/m

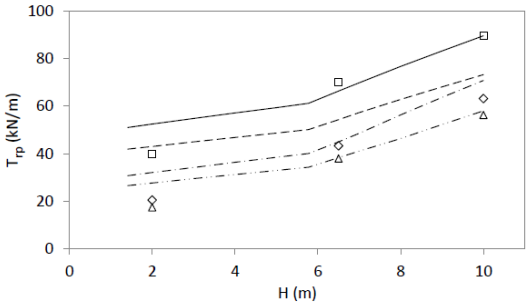

(b) a = 1.0 m, s = 2.0 m, J = 3.0 MN/m

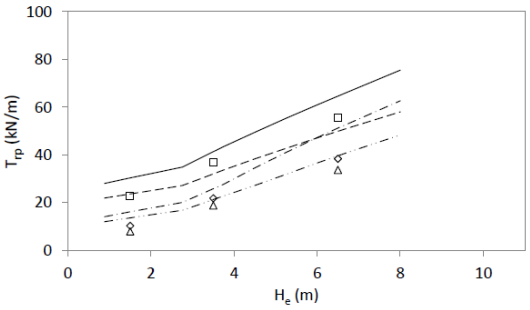

(c) a = 0.5 m, s = 1.25 m, J = 1.0 MN/m

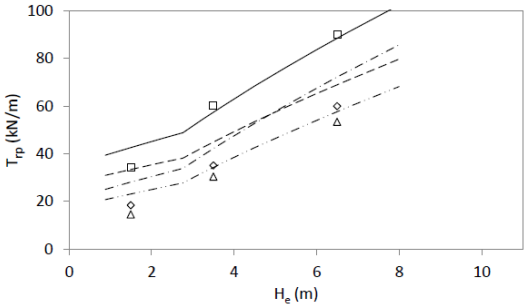

(d) a = 0.5 m, s = 1.25 m, J = 3.0 MN/m

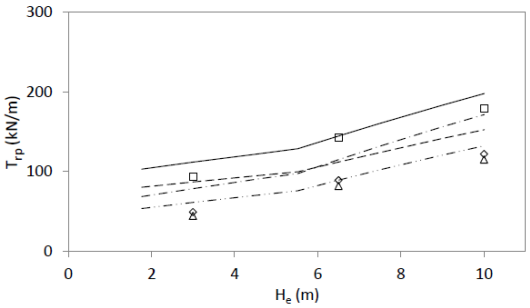

(e) a = 1.0 m, s = 2.5 m, J = 3.0 MN/m

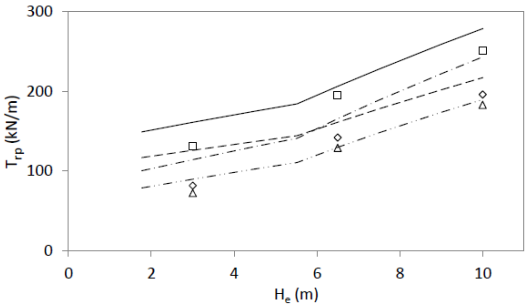

(f) a = 1.0 m, s = 2.5 m, J = 10 MN/m

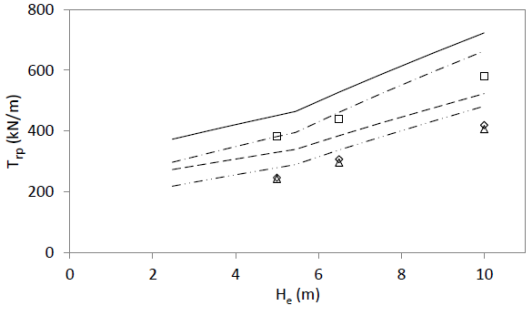

(g) a = 1.0 m, s = 3.5 m, J = 10 MN/m

Figure 4 - Variation of reinforcement tension (T_{rp}) with embankment height (H_e): BS8006 predictions (including proposed modification for subsoil) and FE results